



Investigation of electrical conductivity and optical absorption in amorphous InXSe100-X alloys

A. Maan, D. Goyal, Sachin Sharma, T. Sharma

► To cite this version:

A. Maan, D. Goyal, Sachin Sharma, T. Sharma. Investigation of electrical conductivity and optical absorption in amorphous InXSe100-X alloys. *Journal de Physique III*, 1994, 4 (3), pp.493-501. 10.1051/jp3:1994141 . jpa-00249118

HAL Id: jpa-00249118

<https://hal.science/jpa-00249118>

Submitted on 4 Feb 2008

HAL is a multi-disciplinary open access archive for the deposit and dissemination of scientific research documents, whether they are published or not. The documents may come from teaching and research institutions in France or abroad, or from public or private research centers.

L'archive ouverte pluridisciplinaire **HAL**, est destinée au dépôt et à la diffusion de documents scientifiques de niveau recherche, publiés ou non, émanant des établissements d'enseignement et de recherche français ou étrangers, des laboratoires publics ou privés.

Classification

Physics Abstracts

72.15C — 72.80N — 78.40 — 78.65

Investigation of electrical conductivity and optical absorption in amorphous $\text{In}_x\text{Se}_{100-x}$ alloys

A. S. Maan ⁽¹⁾, D. R. Goyal ⁽¹⁾, Sachin K. Sharma ⁽²⁾ and T. P. Sharma ⁽²⁾

⁽¹⁾ Physics Department, Maharshi Dayanand University, Rohtak - 124 001, Haryana, India

⁽²⁾ Department of Physics, Meerut University, Meerut - 250 004, India

(Received 30 June 1993, revised 10 December 1993, accepted 14 December 1993)

Abstract. — Results related to the d.c. conductivity made over a wide temperature range (130-380 K) in amorphous thin films of various glassy compositions of $\text{In}_x\text{Se}_{100-x}$ alloys are presented in this paper. D.C. conductivity in present set of glasses comprises of three well-known regions and from these observations a number of parameters have been calculated. The conduction has been discussed in terms of known transport mechanisms. Also included are the optical absorption studies in thin films of the present set of alloys. These measurements have been made on the as prepared and annealed samples. The annealing of samples has an important effect on the optical properties and causes a reduction in the energy range of tail states, thus an increase in the optical energy gap in all the alloys. The mechanism of optical absorption seems to follow the rule of non-direct transitions. The results obtained for different samples are compared with each other and reasonable curves for optical absorption are found.

Introduction.

Carrier transport and recombination processes are of fundamental importance to understand optoelectronic properties in amorphous substances as well as of physical interests in fully disordered systems. In-Se glasses have proved to be attractive candidates in optical and electronic communication, switching and memory devices and photovoltaic applications. In-Se films have been demonstrated to work as an excellent device for solar energy conversion [1] with an efficiency as high as 18 %.

Amorphous films of In-Se also exhibit anomalous features compared with other chalcogenide glasses which make them more interesting to study. They show negative Seebeck coefficient in certain compositions [2] unlike other chalcogenides which are generally p-type. They also show large Fermi level shift [2-4], although, the Fermi level in amorphous chalcogenides is said to be pinned near the middle of the gap. An anomalous rise [5] of photocurrent in these glasses is also reported. Moreover, they have an energy gap [6] and a mobility of majority carriers almost of the same order as those of the crystalline Si or GaAs and thus have close optical and transport properties.

Properties like structural properties [2], photoconduction [5-7], X-ray absorption [8], photovoltaic properties [1, 9-11], mobility [12], switching and memory [13], a.c. conduction

[14, 15] and optical absorption [2-4, 16-18] have already been reported. Giulio *et al.* [17] have studied the effect of thermal annealing on optical absorption in InSe and reported that annealing increases the optical band gap. Watanabe and Yamamoto [2] have reported the optical band gap in amorphous $\text{In}_x\text{Se}_{100-x}$ system over a wide range of compositions i.e. $x = 6\%$ to 60% and observed a large difference between optical and electrical band gap. However, the results reported in various papers are very different from each other.

In the present work an effort has been made to analyze the process of charge transport in different compositions of the $\text{In}_x\text{Se}_{100-x}$ system ($x = 10, 15, 20, 25$) over a wide range of temperature (130-380 K). The d.c. conduction in the present set of glasses presents three distinct processes in different temperature ranges. Also carried out are the measurements of optical absorption in as-deposited and annealed thin films of all the four compositions in the range 380 nm-760 nm. It has been observed that annealing has a strong effect and the optical absorption decreases with annealing in all the alloys.

Experimental details.

The different compositions of the glassy $\text{In}_x\text{Se}_{100-x}$ alloys were prepared in bulk form by the quenching technique using elemental constituents of five-nines purity in desired stoichiometric ratios. X-ray diffraction pattern of the samples were obtained, which confirmed the glassy nature of the material.

Bulk as-obtained was further used for the preparation of the planar thin film samples used in the study of the d.c. conductivity by the vacuum evaporation technique. Indium electrodes onto a well degassed corning glass slide were deposited by the vacuum evaporation technique prior to the deposition of the sample under investigation. The thickness of the film was monitored on a VICO digital thickness monitor using a quartz crystal and varies in the range 0.1-0.5 μm for various compositions. The thin film samples were annealed in dark under vacuum (10^{-2} Torr) at 380 K, for about 2 hours before the measurement of d.c. conductivity.

The conductivity measurements were carried out on the annealed thin films by holding the films in a metallic cryostat. The low temperatures were attained by cooling the samples using liquid nitrogen and subsequently an experimental run up to 380 K was performed for each composition. A d.c. bias of 10 V was applied across the sample and current measurements were made using a programmable 617 Keithley Electrometer.

For optical absorption studies, planar films of different compositions having thickness ranging from 0.3 to 0.5 μm were prepared by vacuum evaporation. Their optical absorption was measured using a Hitachi 3400 computerised spectrophotometer with double monochromator. The spectrophotometer plots the result as $\alpha \cdot t$ vs. wavelength, where t is the thickness of the films and α is the absorption coefficient. These studies were made on both the as deposited and annealed samples. For the later the films were annealed at 380 K for one hour under a vacuum of 10^{-2} Torr in the absence of light.

Results and discussion.

In non crystalline materials, the transport mechanism due to hopping of charge carriers are different from the usual conduction processes in the sense that the carrier transport takes place in the localized energy region within the forbidden gap. Using the concept of Mott and Davis [19], three different mechanisms contribute to the charge transport in these materials. (I) Conduction by carriers excited into extended states, (II) conduction in band tails due to thermally activated hopping and (III) conduction in the localized states at the Fermi energy.

Temperature dependence of the d.c. conductivity has been observed in all the four compositions in the temperature range (130-380 K). Figure 1 shows the variation of

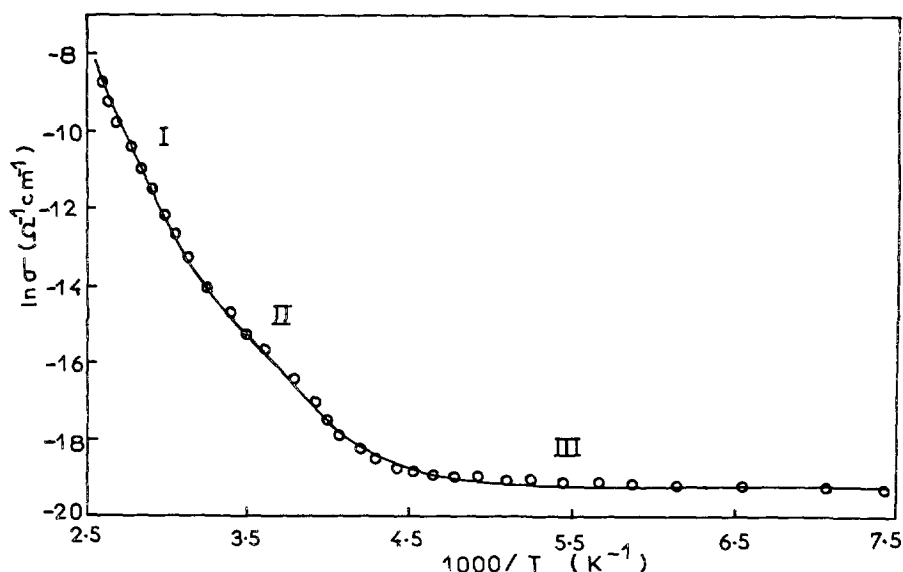


Fig. 1. — The temperature dependence of conductivity plotted as $\ln \sigma$ vs. $1000/T$ for $\lambda = 25$ alloy.

$\ln \sigma$ in $\lambda = 25\%$ alloy as a function of $1000/T$. The results obtained in other three compositions are similar in nature. From the data plotted in figure 1, it can be clearly seen that the conduction in present set of alloys can also be divided in three distinct regions.

The high temperature range i.e. above room temperature (300 K) is clearly distinguishable from the two mechanisms active in the low temperature range. $\ln \sigma$ vs. $1000/T$ plot is clearly linear in region I and indicates that d.c. conductivity is an activated process with single activation energy. An exactly similar behaviour has been observed in all other compositions as well. The activation energy (ΔE_1) of dark carriers in this region has been computed from the experimental data for different compositions and are inserted in table I.

In region I, with increasing temperature the probability of thermal emission of charge carriers to the permitted zone increases and is the dominant process at temperatures larger than 300 K. The charge transport in present set of glasses seems to follow the relation [19]

$$\sigma = \sigma_0 \exp. (-\Delta E_1/kT) \quad (1)$$

Table I. — Various parameters related to d.c. conductivity and optical absorption measurements in different compositions of the $\text{In}_\lambda\text{Se}_{100-\lambda}$ system.

Composition λ	ΔE_1 (eV)	ΔE_2 (eV)	σ_0 $\Omega^{-1} \text{cm}^{-1}$	N_{E_1} $\text{eV}^{-1} \text{cm}^{-3}$	R (Å)	T_0 (K)	E_0 (eV)	
							Unannealed	Annealed
10	0.79	0.33	3.9×10^4	5.9×10^{21}	16.3	3.16×10^4	1.18	1.58
15	0.58	0.22	2.8×10^3	2.1×10^{21}	21.2	9.02×10^4	0.98	1.20
20	0.54	0.18	1.7×10^3	3.4×10^{20}	33.3	5.51×10^5	0.94	1.15
25	0.68	0.37	5.3×10^4	7.7×10^{21}	15.2	2.39×10^4	1.14	1.40

where σ is the electrical conductivity, σ_0 is the preexponential factor and ΔE_1 corresponds to the activation energy. Out of various conduction mechanisms for d.c. conductivity in chalcogenide glasses, the conduction by charge carriers excited into extended states just above E_c or just below E_v is governed by the relation given above. The constant σ_0 is generally equated with σ_{\min} , the smallest non-zero value of conductivity at absolute zero [19]. Typical value of this constant has been predicted to be of the order of $10^3 \sim 10^4 \Omega^{-1} \text{cm}^{-1}$. Using the relation given above, values of the preexponential factor have been calculated for each sample and are given in the table. One can clearly see from the table that the values of the preexponential factor are strikingly in good agreement with the above-discussed conduction mechanism, and decrease with increasing In % with the exception of $x = 25$ sample where it again increases.

From the data in figure 1, it can be seen that the conduction in region II is clearly different from that of region I and can be attributed to the transport of carriers excited into the tails of localized states and migrating by a hopping mechanism as given below.

$$\sigma \propto \exp \cdot \{ - (\Delta E_2/kT) \} \quad (2)$$

where ΔE_2 is the activation energy for the region II and is a measure of the extent of tailing of the band states [19]. The activation energy for hopping due to this mechanism has been calculated and comes out to be 0.37 eV for the $x = 25$ sample. Values of activation energies for other compositions are also calculated from the experimental data and are listed in the table.

At low temperatures, the conduction can be attributed to the hopping of charge carriers between the neighbouring centres at the Fermi energy. The hopping conduction according to Mott [19] can be expressed as,

$$\sigma \propto \exp \cdot (-W/kT) \times \exp \cdot (-2R/a) \quad (3)$$

where W is the energy difference between the localized states between which the hopping takes place, R is the hopping distance and a is the radius of localization and $1/a$ is the quantity representative for the rate of fall off of the wave function at a site. With the lowering of temperature the number and energy of phonons decrease, and the more energetic phonon assisted hops will become progressively less favorable. In such a case (region III), the conductivity has even lesser temperature dependence and the hopping of the charge carriers takes place through a greater distance but to an energy nearer to that of the centres. This mechanism is the so-called variable range hopping. Thus one can conclude that the hopping occurs between the states in the narrow energy band near the Fermi level and the conductivity can be expressed as [19],

$$\sigma \propto \exp \cdot (T_0/T)^{1/4} \quad (4)$$

where T_0 is a constant and is equal to $16/N_{\text{Et}} \cdot k \cdot a^3$. Here N_{Et} denotes the density of states near the Fermi level and k is the Boltzmann's constant. The conductivity in this region, in accordance with relation (4) obeys the $T^{-1/4}$ law. With a view to have a comparative look, the experimental data for different compositions are plotted in figure 2 on $T^{-1/4}$ scale. In present set of glasses, the $T^{-1/4}$ law applies for temperatures $T < 225 \text{ K}$: which can be clearly seen from the plots in figure 2. Also it can be observed that the $T^{-1/4}$ law makes the conductivity quite insensitive to temperature variations. In the low temperature regime, it has been established that $T^{-1/3}$ and other T functions also achieve the same linearity in $\ln \sigma$ [20]. In a similar way plots of $\ln \sigma \sqrt{T}$ vs. $T^{-1/4}$ [21-23] have also been observed to be linear in this temperature range, which prove the insensitivity of the conductivity on temperature ($\ln \sigma$ vs. $T^{-1/n}$ plots), with n varying from three to six. Different indices such as $1/3$, $1/4$ are often associated with the dimensionality of the electron transport [20].

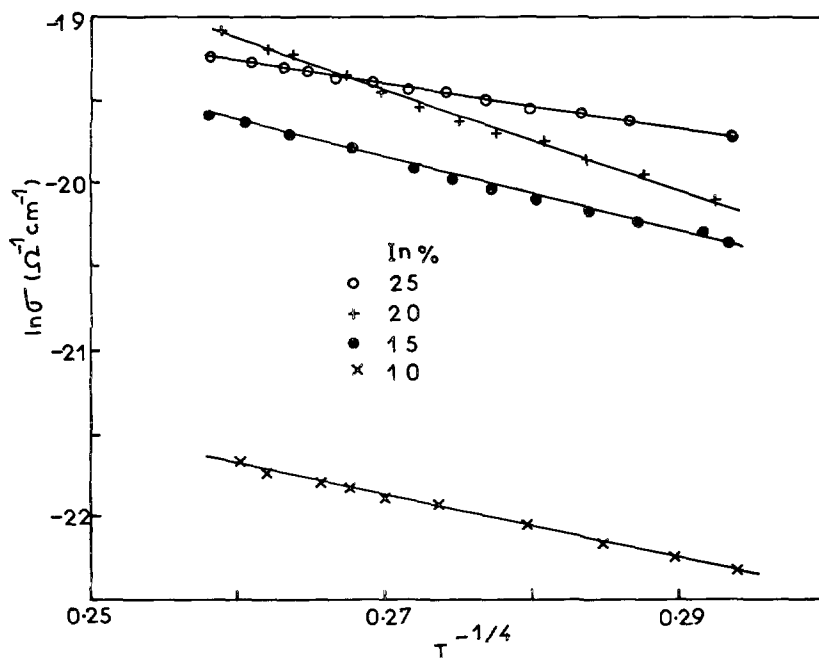


Fig. 2. — The temperature dependence of conductivity in low temperature region plotted as $\ln \sigma$ vs $T^{-1/4}$ for different alloys.

The data presented in figure 2 have been used to calculate the density of states N_{El} at the Fermi level using the relation (4). Constant T_0 has been evaluated from the slope of the $\ln \sigma$ vs. $T^{-1/4}$ plots and is listed in the table for all the four alloys. Using the relation $T_0 = 16/a^3 kN_{\text{El}}$ as mentioned before, N_{El} values have been obtained by assuming the radius of localization as 10 Å. Also evaluated is the hopping distance R of the charge carriers [24] given as,

$$R = (9/8 \pi N_{\text{El}} kT)^{1/4} \quad (5)$$

and is between 15 and 33 Å, as shown in the table. The hopping distance has been found to decrease with increasing temperature. Thus from the experimental results in the present system, one can clearly see that the charge transport in the low temperature range can be attributed to the hopping of the charge carriers at the localized states.

It may be mentioned here that Wood *et al.* [3] have reported the variable range hopping in the $\text{In}_x\text{Se}_{100-x}$ system only for the samples with $x > 46$. For $x < 46$ they could observe only the activation type conduction in these alloys. Watanabe and Yamamoto [2] carried out the measurements in the $\text{In}_x\text{Se}_{100-x}$ system over a wide range of compositions from $x \approx 6$ to $x \approx 53$ % and could observe only activated type conduction in all the samples. However, in their later communication [15] they repeated their measurements of d.c. conductivity on $x \approx 37, 40$ and 43 % samples over a wider temperature range and could observe the variable range hopping conduction in these samples.

The identification of optical absorption and other related optical processes occurring at energies below the energy gap E_g with the presence of intrinsic, disorder induced localized state is still not very clear. Although it is not that foolproof, the first test for this classification is the simple requirement that the optical processes be unique to the amorphous state. In

chalcogenide glasses, a typical absorption edge can be broadly ascribed to either of the three processes : (i) residual below gap absorption (ii) Urbach tails and (iii) inter-band transitions. Chalcogenide glasses have been found to exhibit highly reproducible optical edges which are relatively insensitive to preparation conditions and under equilibrium conditions only the observable absorption [25] within the gap accounts for process I. In the second mechanism, the absorption edge depends exponentially on energy, the absorption coefficient $\sim 10^2 \text{ cm}^{-1}$ and increases exponentially with photon energy according to the so-called Urbach relation (26) as :

$$\alpha \sim \exp \cdot \{ \rho (h\nu - h\nu_0)/kT \} \quad (6)$$

where ρ is a constant of order unity, ν_0 is a constant corresponding to the lowest excitonic frequency. On the other hand for α in the range $\sim 10^4 \text{ cm}^{-1}$ it obeys the rule of non direct transitions and is given by the relation

$$\alpha = B (h\nu - E_0)^2/h\nu \quad (7)$$

where $h\nu$ is the incident photon energy, B is the constant determined by the extent of the tail states and E_0 is the optical energy gap.

Figure 3 depicts the variation of $\alpha \cdot t$ with photon energy in various as-deposited samples of the present glassy system. The parameter $\alpha \cdot t$ has been obtained directly from the observations on the Hitachi spectrophotometer. Same data have been used to study the variation of $\sqrt{\alpha h\nu}$ vs. $h\nu$ and the plots for the as-deposited films are depicted by figure 4. From the plots in figure 4 one can see at a glance that the absorption in present set of glasses seems to be due to non direct transitions and the extrapolation of the linear portion of the curve has been used to find out the optical energy gap. The value of the energy gap for as-prepared films of all the four compositions is given in table and one can clearly observe that the E_0 values decrease with increasing In concentration up to $x = 20$ and again increases for $x = 25$ % composition. The present trend, although it is quite similar to that of the activation energy of d.c. conduction, is still not understandable from the present set of experiments.

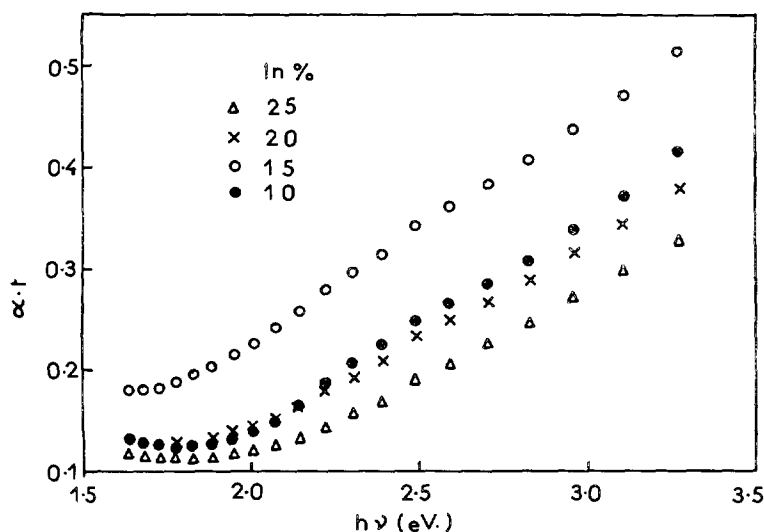


Fig. 3. — Variation of $\alpha \cdot t$ as a function of photon energy in various unannealed compositions of $\text{InSe}_{1(100-x)}$ system.

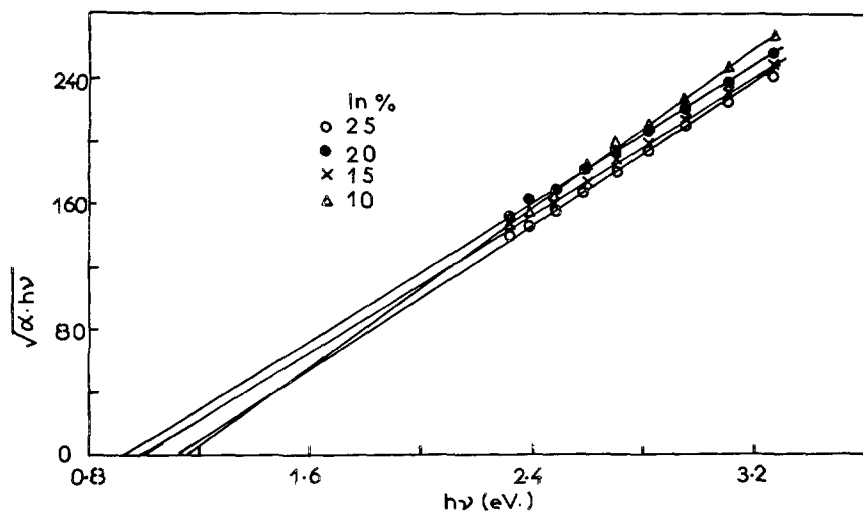


Fig. 4. — Variation of $\sqrt{\alpha \cdot h\nu}$ as a function of photon energy in various unannealed compositions of $\text{In}_x\text{Se}_{100-x}$ system.

In order to have a comparative view of annealing on optical absorption, figure 5 depicts the variation of $\sqrt{\alpha \cdot h\nu}$ vs. photon energy in as-deposited and annealed films of $x = 25$ composition. As discussed earlier relation (7) holds in the higher coefficient region and the extrapolation of the linear portion to the horizontal axis determines the optical energy gap (E_0). One can observe very clearly that the annealing causes an increase in the optical energy gap indicating a reduction in disorderness of the atomic bonding between neighbours and thus

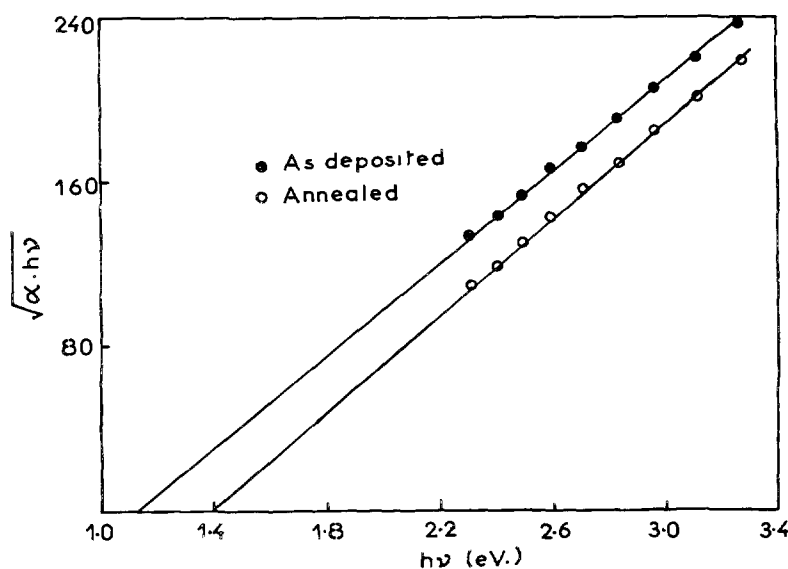


Fig. 5. — Variation of $\sqrt{\alpha \cdot h\nu}$ as a function of photon energy in as deposited and annealed films of $x = 25$ alloy.

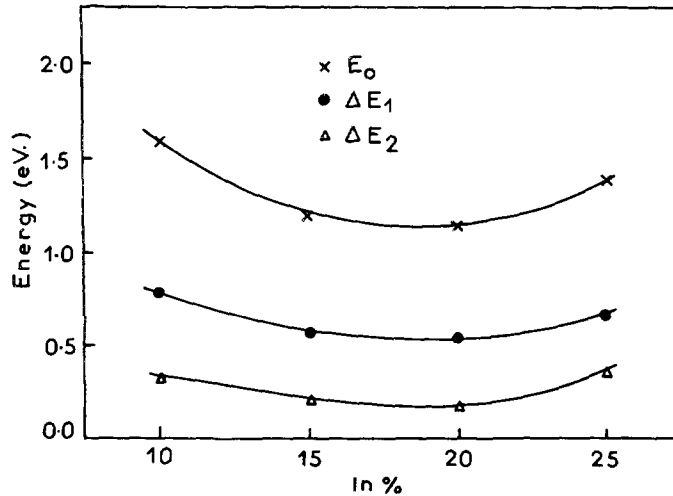


Fig. 6. — Compositional dependence of the parameters obtained from the d.c. conductivity and optical absorption in different alloys.

a shrinkage of the extent of tail states adjacent to the band edge. Similar measurements have been made in all the four compositions and the values of optical band gap have been calculated and are presented in the table.

In order to compare the results of d.c. conductivity and optical absorption data, different parameters (ΔE_1 , ΔE_2 and E_0) are plotted in figure 6 with In %. The figure clearly shows that the three parameters decrease with increasing In % with the lowest value at $x = 20$ %. The value of all these parameters again increases for $x = 25$ alloy. A similar variation with In % has been observed in the parameters such as activation energies for photoconduction and effective decay time constant obtained from the photoconductivity measurements reported elsewhere [27].

Conclusions.

Experimental results of the conduction in various alloys of amorphous $\text{In}_x\text{Se}_{100-x}$ indicated the presence of three distinct regions in the scanned temperature range (130-380 K). Analysis of the results leads to the conclusion that for low temperature i.e. below 300 K, the main contribution is due to the hopping of charge carriers excited into the tails of localized states within the forbidden energy gap. The activation energy for hopping conduction (ΔE_2) has been calculated and shows a minimum for $x = 20$ alloy. In the high temperature region, $T > 300$ K, extended state conduction accounts for all the compositions. The activation energy for extended state conduction (ΔE_1) exhibits a similar compositional dependence as ΔE_2 . Different parameters such as density of states at the Fermi energy (N_{EF}) and hopping radius, etc. have been calculated and are in fair agreement with the theory.

It has been observed that annealing has an important effect on the optical gap which increases with annealing. Such a behaviour indicates a reduction in the disorderness of atomic

bonding between neighbouring atoms and shrinkage of the extent of tail states adjacent to the band edges.

Acknowledgments.

Financial support by the U.G.C. during the course of work is gratefully acknowledged.

References

- [1] Ando K. and Katsui A., *Thin Solids Films* **76** (1981) 141.
- [2] Watanabe I. and Yamamoto T., *Jpn J Appl Phys* **24** (1985) 1282.
- [3] Wood C., Gilbert L. R., Garner C. M. and Shaffer C., Proc. 5th International conf. Amorphous and liquid Semiconductors (Taylor and Francis, London, 1974) 1, p. 285.
- [4] Nang T. T., Matsushita T., Okuda M. and Suzuki A., *Jpn J. Appl Phys* **16** (1977) 253.
- [5] Maan A. S., Goyal D. R. and Kumar A., *J Non Cryst. Solids* **110** (1989) 53.
- [6] Di Giulio M., Micocci G., Rella R., Siciliano P. and Tepore A., *Thin Solid Films* **148** (1987) 279.
- [7] Maan A. S., Goyal D. R. and Kumar A., *J Mater Sci Lett* **7** (1988) 1384.
- [8] Kumar Arvind, Hussain M., Swarup S., Nigam A. N. and Kumar A., *X-ray Spec.* **19** (1990) 27.
- [9] Matsushita T., Suzuki A., Okuda M., Naitoh H. and Nakau T., *Jpn J Appl. Phys* **22** (1983) 762.
- [10] Matsushita T., Suzuki A., Okuda M. and Sakai T., *Jpn J Appl Phys* **19** (1980) 123.
- [11] Segura A., Besson J. M., Chevy A. and Martin M. S., *Il Nuovo Cemento B (Italy)* **38** (1977) 345.
- [12] Okuda M., Krimoto T., Naito H., Matsushita T. and Nakau T., *J. Non Cryst Solids* **59 & 60** (1983) 1035.
- [13] Grindle S. P., *J Appl Phys (USA)* **51** (1980) 5464.
- [14] Di Giulio H., Rella R. and Tepore A., *Phys Status Solidi (a)* **100** (1987) 35.
- [15] Watanabe I. and Sekiya T., *Jpn J Appl Phys.* **26** (1987) 633.
- [16] Sharma T. P., Sharma S. K., Kumar R. and Jain Garima, *Ind J. Pure Appl Phys* **28** (1990) 486.
- [17] Di Giulio M., Manno D., Rella R., Siciliano P. and Tepore A., *Sol Energy Mater* **15** (1987) 209.
- [18] Chaudhuri S., Biswas S. K. and Choudhuri A., *Solid State Commun* **53** (1985) 273.
- [19] Mott N. F. and Davis E. A., *Electronic Processes in Non Cryst. Materials* (Clarendon Press Oxford, 1979).
- [20] Maschke K., Overhof H. and Thomas P., *Electronic and Structural Properties of Amorphous Semiconductors* (London. Academic, 1974) p. 141.
- [21] Mott N. F., *J Non Cryst Solids* **8-10** (1972) 1
- [22] Brodsky M. H. and Gambino R. J., *J Non Cryst. Solids* **8-10** (1972) 739.
- [23] Bluzer N. and Bahl S. K., *Amorphous and Liquid Semiconductors V.1* J. Stuke and W. Brenig Eds. (London, Taylor and Francis, 1974) p. 31.
- [24] Nagels P., *Amorphous Semiconductors*, M. H. Brodsky Ed. (Springer Verlag, New York, 1979) Ch. 6, p. 126.
- [25] Tauc J., *Amorphous and liquid Semiconductors*, J. Tauc Ed. (Plenum, New York, 1974) p. 159.
- [26] Urbach F., *Phys Rev* **92** (1953) 1324.
- [27] Maan A. S. and Goyal D. R., *Communicated to J Phys. Condensed Mater*